Cation-Alloying as a Pathway to Reproducible Solution-Based Preparation of Efficient Metal Halide Perovskites Solar Cells with Increased Stability

Michael Saliba[1]* and Eva L. Unger[2,3]*

[1] Swiss Federal Inst. of Technology (EPFL) Lausanne, Switzerland
[2] Helmholtz-Zentrum Berlin für Materialien und Energie GmbH, Germany
[3] Lund University, Sweden

ABSTRACT

With a certain amount of serendipity, research on dye-sensitized solar cells led to the discovery of metal halide perovskite semiconductors as a solar energy conversion material[1,2] that has inspired world-wide research activities leading to efficiency increases from about 10% in 2012[3,4] to now 22%.[5–8] Apart from their use as a single junction solar cell technology, metal halide perovskites can be processed as an add-on layer onto other solar cells to realize efficient and low-cost tandem architectures. The perovskite band gap can be tuned continuously from 1.1 to 3.0 eV by chemical engineering which makes them particularly relevant for multi-junction devices.[9–12] Experimental demonstrations of efficient tandem devices comprising metal-halide perovskites as one[13–15] or both[10,16] components in a tandem stack highlight the potential for scalable and low-cost multi-junction devices[17] with efficiencies approaching 30% is considered feasible.[18,12,19,20]

To reach this performance in a perovskite/silicon tandem, the ideal band gap of the absorber material in top device should be about 1.7 eV[18,12,21] (sine silicon has a band gap of 1.1 eV).[11,22,23] In this review, we dedicate section I to the discussion of the chemical tunability of metal halide perovskite with a particular focus on absorber materials with absorption onsets[i] around 1.6 eV. Section II reflects on the benefit and role of including cesium (Cs) highlighting the work by Saliba et al.[5,6] as this approach demonstrates a reliable pathway to obtain efficient solution-processed metal halide perovskite absorbers with high reproducibility and extended operational device stability. Section III focuses on the state-of-the art of perovskite photovoltaics as a function of the absorption onset of the absorber layer highlighting materials with band gaps between 1.6 eV-1.75 eV as these are of great importance to the development of efficient tandem solar cells.[12,18–20] In the conclusion section IV, we reflect on more general trends in metal halide alloys partially discussed elsewhere[23] highlighting cation-alloying as an approach to obtain highly efficient devices in the band gap range between 1.6 and 1.7 eV.

The data shown and discussed here is dominantly based on three of our recent publications and the interested reader is kindly referred to Unger et al.[23] and Saliba et al.[5,6] for more in-depth discussions and experimental details.

I. BAND GAP TUNING IN METAL HALIDE PEROVSKITE ALLOYS

Hybrid metal halide perovskites containing methylammonium (MA) molecules as central cations in three-dimensional lead-[24] or tin-halide[25] perovskites were first synthesized and characterized by Weber in 1978. The different colors of crystals synthesized in these first results indicated that the optical properties varied with the halide substitution from Cl, Br, to I. In 2012, Noh et al.[9] confirmed a tuneable band gap by halide substitution in the $MAPb(Br_xI_{1-x})_3$ series. Since then, alloying has become a valuable approach to tune the absorption onset e.g. by substituting iodide with bromide[9,26,27], or lower band gaps towards the infrared in lead-tin alloyed perovskites.[10,28–30] The latter is also motivated by the necessity to find alternatives not containing lead as this might be one main obstacle in the commercialization of perovskite solar cells.

Another important aspect driving the investigation of various alloys is the search for more stable perovskite semiconductors because the MA cation is proving to be a volatile component making the material prone to photochemical, thermal, and humidity induced degradation.[31,32] Cation-alloys comprising methylammonium (MA)[26,9,33,34], formamidinium (FA)[11,27,35], cesium (Cs)[5,36,37] and also rubidium (Rb)[6,38] have led to devices with better reproducibility, morphology, performance, and stability. The data sets compared here stem from a range of different ABX_3 compounds where A can be a monovalent organic cations such as $MA^{+9,26,39}$ or $FA^{+11,40}$, inorganic cations such as cesium (Cs^+), or a mixture of these.

The Goldschmidt tolerance factor, although introduced for oxide perovskites,[41] has been proven to be a useful tool to empirically estimate form-ability also for halide perovskites.[6,35,42] Tolerance factor considerations are also useful in the rationalization of experimental trends in perovskites and aid in engineering of alloys with e.g. higher stability and we here show estimated tolerance factors of lead-based perovskites as a function of the cation as well as anion radii in Figure 1 (left).
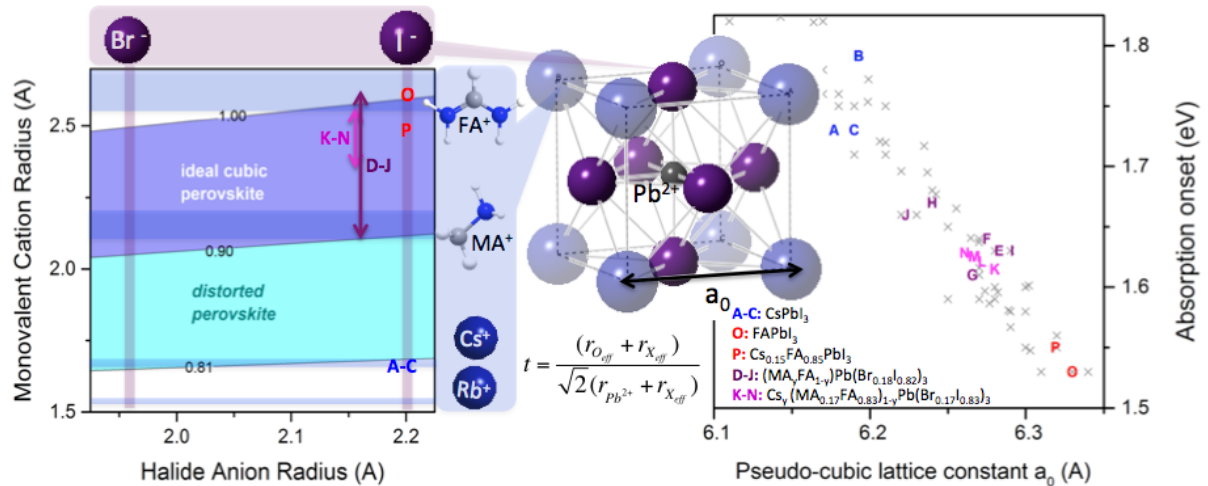
Figure 1: (left) Goldschmidt tolerance factor estimation as a function of cation and anion radius for lead-based perovskite materials. (middle) Crystal structure of (pseudo-)cubic metal halide perovskite with Pb^{2+} depicted as central ion. (right) Correlation of the experimental absorption onset of various metal halide alloys as a function of the metal halide perovskite pseudo-cubic unit cell lattice parameter a_0. Data points shown in grey are further discussed in Ref [23].

As an example for the value of tolerance factor considerations, we highlight metal halide perovskites comprising FA as well as the purely inorganic Cs-based metal halide perovskites

that have a substantially higher thermal stability compared to methylammonium-based compounds. However, both tend to form non-perovskite crystal phases at room temperature that are "yellow" due to their lack of semiconductor properties.[35,43,44] Tolerance factor estimations place FAPbI$_3$ (O in Figure 1) at a value slightly too high to form stable cubic perovskites and experiments prove that a non-perovskite trigonal phase is the thermodynamically more stable phase at room temperature. CsPbI$_3$ (A in Figure 1) on the other hand is predicted not to form as the Cs-cation is too small to stabilize a perovskite crystal structure. Mixing cations is hence a mean to adjust the effective cation size leading to perovskite alloys with a more favorable tolerance factor.[5,34,43,44] For pure bromide lead perovskites, both the MA and Cs derivate can be obtained (as the tolerance factor is more favorable for CsPbBr$_3$, see Figure 1, left) suggesting that the methylammonium cation does not affect material properties relevant for solar cell device operation.[31]

Besides determining whether or not a stable perovskite phase can form, the dimensions of constituent ions also directly determine the perovskite lattice dimensions which, in turn, determines the absorption onset of the resulting perovskite alloy, shown in Figure 1 (right). The data depicted with crosses in the background is part of the data set discussed elsewhere[23] and we here chose to specifically highlight trends in cation alloys in the narrow band edge range between 1.5 and 1.8 eV. The plot shows that both the purely inorganic CsPbI$_3$ compounds as well as FAPbI$_3$ fall on a similar general trend-line for Pb-based ABX$_3$ alloys for different cations or cation-alloys as well as bromide/iodide anion alloys. As both these materials only form meta-stable perovskite structures, the data point for the pure FAPb(Br$_{0.18}$I$_{0.82}$)$_3$ (point D) were outside the displayed data range of Figure 1 and literature values for pure CsPbI$_3$ may vary strongly dependent on the degree of material degradation to the non-perovskite phase.

Alloys of MA and FA[34] and MA/FA alloys incorporating Cs[12] (triple cations) are found to follow the trend of absorption onset as a function of the pseudo-cubic lattice constant a_0 closely (Figure 1, right).[ii] For the data sets of (MA$_y$FA$_{1-y}$)Pb(Br$_{0.18}$I$_{0.82}$)$_3$ (with y = 0% (D), 18% (E), 33% (F), 50% (G), 67% (H), 82% (I) and 100% (J)), the data points follow roughly the predicted trend line but exhibit some scattering in the experimental data points that could be caused by slight compositional inhomogeneity of cation and halide anion distribution in the ABX$_3$ absorber. Increasing the amount of Cs in Cs$_y$(MA$_{0.17}$FA$_{0.83}$)$_{1-y}$Pb(Br$_{0.17}$I$_{0.83}$)$_3$ (with y = 0% (K), 5% (L), 10% (M) and 15% (N) in Figure 1) the lattice dimensions and absorption onset are found to decrease according to the predicted trend (K-N in Figure 1, right). Cs incorporation is hence found to obey the trend-line established for hybrid perovskite semiconductors incorporating MA and FA opposed to the statement made previously.[23,ii] The amount of Cs that can be included in the structure seems limited as no stable perovskite materials are found to form for Cs concentration exceeding 15%, above which, phase-segregation and formation of "yellow" phases rather than perovskite semiconductor phases seem to be favored.[5,44,45]

Overall, we find that cation alloying, irrespective of whether organic or inorganic cations are used,[ii] follow a similar trend-line suggesting that the optical properties at the absorption onset are determined by the lattice dimensions. This insensitivity of the band-to-band electronic transition on the chemical nature of the cation and that the cation merely determines the lattice dimensions is expected from theoretical calculations. These predicted the band-to-band electronic transitions to be solely determined dominated by the Pb-6s and I-5p orbitals (valence band maximum) and Pb-6p orbitals (conduction band minimum) with no electronic influence from the central monovalent cation.[46,47] Hence, it is mainly the metal-halide cage that determines the optoelectronic properties of perovskites.

II. ROLE OF ALKALINE IONS IN CATION-ALLOYS

The addition of alkaline ions such as Cs[5,6,43,45] and Rb[6,38] to hybrid MA or FA-based lead halide perovskites has advantageous effects on the semiconductor properties due to tolerance factor adjustments as discussed in the previous section. Even the largest alkaline cation, cesium, has an ion radius bordering "too small" to form stable perovskites by itself but can favorably be used to tune the tolerance factor by partial substitution of the larger organic MA and FA cations as discussed in the previous section.

From the blue shifted PL and decreased lattice parameter a_0 found from XRD analysis, it can be concluded that Cs is included. The PL shift in addition is relatively linear which is consistent with full inclusion of Cs. The absolute amount of Cs inclusion into the crystal lattice is currently under investigation. The X-ray diffractograms shown for these materials in Figure 2 (right) clearly indicate the contraction of the cubic lattice upon addition of cesium from a_0 = 6.28 Å for $(MA_{0.17}FA_{0.83})Pb(Br_{0.17}I_{0.83})_3$ to a_0 = 6.26 Å for $Cs_{0.15}(MA_{0.17}FA_{0.83})_{0.85}Pb(Br_{0.17}I_{0.83})_3$. Besides the slight change in lattice constants, the qualitative comparison of the experimental diffractograms also shows a relative increase of the 110 and 210 reflections compared to the main 100 and 200 peaks.
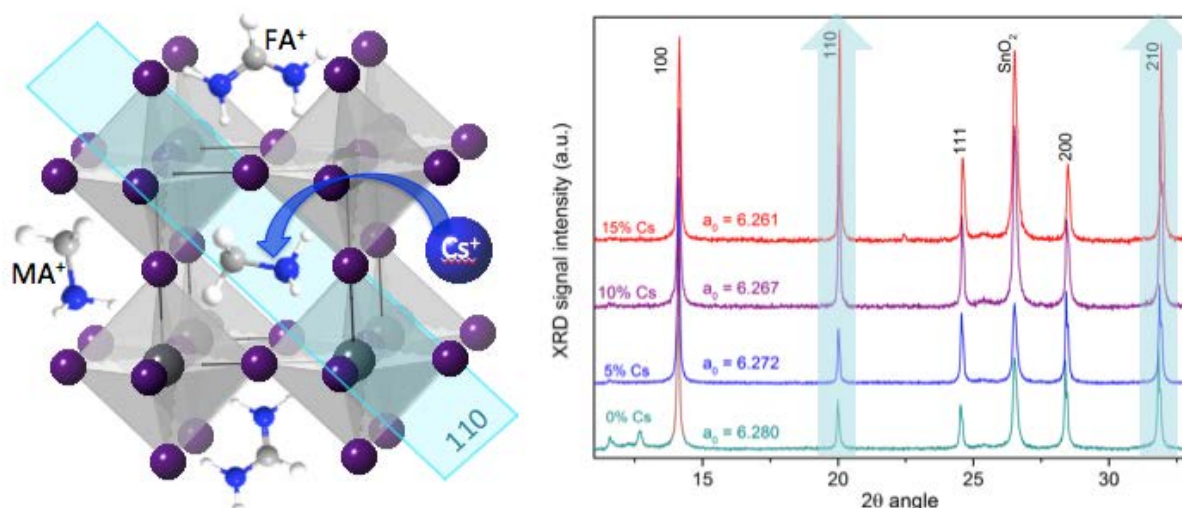
Figure 2: (left) Illustration of Cs incorporation in mixed MA/FA lead halide perovskites with the composition $Cs_y(MA_{0.17}FA_{0.83})_{1-y}Pb(Br_{0.17}I_{0.83})_3$ with indication of the 110 lattice plane that appears to exhibit enhanced scattering upon Cs inclusion in the X-ray diffraction data for varying amount of Cs (0% - 15%) shown on the right side. Full data set shown in Ref [5].

This could indicate a change in the preferential orientation of crystals during growth but is in this case likely due to the substitution of organic cations with Cs as the latter should have a much higher scattering factor due to its elemental mass compared to the organic cations. Interestingly, the ratio between the 100 and 200 peaks seem unchanged whereas reflections from "diagonal" (see illustration in Figure 2, left) lattice planes increase. This suggests that cesium cations do not seem to be preferentially incorporated into adjacent unit cells but rather into unit cells diagonal from each other, which can be expected to be entropically favored. More thorough XRD analysis is needed to illuminate structural details of Cs-inclusion into hybrid perovskites such as site occupancy, which is beyond the scope of this manuscript.

Alkali-cation additives such as Cs not only affect the optoelectronic properties of metal halide perovskites but also influence the film formation. X-ray diffractograms with increasing amount of Cs (Figure 2, right) provide evidence that fewer impurity phases such as PbI_2 (reflection peak at 12.6) are present. Also, UV-Visible absorption data and X-ray diffractograms prove metal halide perovskite semiconductor formation without any annealing when Cs is present in the wet film. Even highly efficient devices could be made from such films without annealing.[5,48] Cross-section scanning electron microscopy images (Figure 4, a and b) suggest a more uniform and monolithic crystal growth for Cs-containing perovskites. Apart from adjustment of the effective cation radii yielding materials with more favorable tolerance factors, alkaline cations also improve the stability and induce more favorable film formation conditions as well as supressing impurity phases.

As an additive, Rb seems to have a similar beneficial effect on metal halide perovskite layer formation but at present the amount of Rb integration is still under debate. It would appear that Rb only incorporates partially and less effectively than Cs. Interestingely, recent XPS studies by Phillipe et al. show that the presence of Cs facilitates more Rb integration into the perovskite grains.[49] Potentially, the slightly lower cation radius and hence even less favorable tolerance factor prevent full Rb-inclusion.[6] Similar to Cs, Rb induces crystallization of the perovskite layer at lower temperature[6,38] and helps to supress impurity phases. As for Cs-containing materials, more thorough material analysis distinguishing the role and beneficial effects on film formation, crystallinity and stability as well as detailed analysis of the amount and distribution of potentially incorporated alkaline cations is needed to illuminate their precise function in metal halide perovskite solar cells.

III. CATION-ALLOYS FOR INCREASED DEVICE EFFICIENCY AND STABILITY

Inclusion of Cs cations in the precursor of solution-processed metal halide perovskite semiconductors has been shown to have a three-fold benefit on the resulting solar cell devices: 1) increased thermal stability, 2) less phase impurities, and 3) higher experimental reproducibility by reducing the impact of processing conditions.[5]

This was established by comparing large data sets for devices comprising none or 5% Cs hence allowing to draw statistically relevant conclusions. The substantial increase of the power conversion efficiency from an average of about 16.5% to 19.5% (Figure 3 c) was dominantly caused by a clear increase in the photocurrent as well as a substantially increased fill factor while the open circuit voltage only shows a slight improvement. These findings allude that the intrinsic metal halide perovskite semiconductor properties improve upon inclusion of Cs in $Cs_y(MA_{0.17}FA_{0.83})_{1-y}Pb(Br_{0.17}I_{0.83})_3$.

Apart from a potentially higher internal quantum yield due to a better crystal quality, the higher short circuit current and fill factor[5] indicate an improved charge carrier collection efficiency. A possible reason might be the absorber layers morphology as Cs-incorporating materials appear to grow more monolithically off the meso-porous TiO_2 layer on the electron-selective fluorine-doped tin oxide substrate (SEM image in Figure 3 b) compared to the material incorporating no Cs at all (SEM image in Figure 3 a). Fewer inter grain boundaries in the direction of current flow are formed which is likely of substantial benefit for charge carrier collection. Cs alkaline cations are interpreted to have a beneficial effect on the crystallization kinetics and film formation of metal halide perovskite layers. Another important aspect is the lack of impurity such as the higher band gap lead iodide, PbI_2, as these might lead to non-beneficial energetic offsets at the titanium dioxide, TiO_2, interface that would make charge carrier extraction at this interface less favorable.

The most important benefit of Cs-containing alloys is their clear increase of the long-term device stability shown in Figure 3 d. This indicates that either Cs improves the intrinsic material stability significantly or that the devices incorporating Cs are less prone to device-related efficiency decline due to e.g. the demise of interfacial properties leading to a substantially reduced charge collection efficiency.
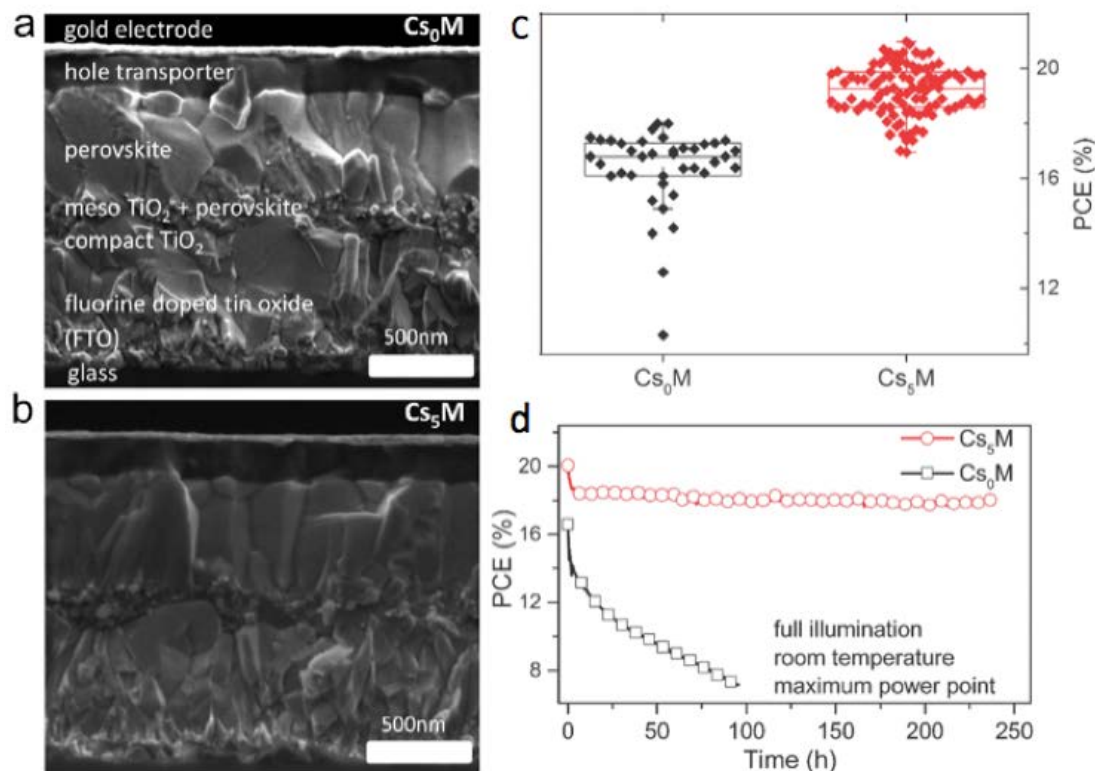

Figure 3: (a & b) Scanning electron microscopy cross section images of device comprising $Cs_y(MA_{0.17}FA_{0.83})_{1-y}Pb(Br_{0.17}I_{0.83})_3$ with 0% (a) and 5% (b) Cs. (c & d) Comparison of the power conversion efficiency (c) and long term stability (d) of devices comprising 0% and 5% Cs. Small amounts of Cs is found to have a beneficial effect on the reproducibility, performance and long term stability of metal halide perovskite solar cells. Data reproduced from Ref [5], published under a CC BY-NC 3.0 creative commons agreement.

The data discussed in detail for Cs-containing perovskites also includes the following overview graph where the device performance metrics are compared as a function of the absorber layer absorption onset. The data points in grey scale are further discussed elsewhere[23] and referenced therein. These overview plots show that single junction devices are approaching theoretical performance limits and especially for devices with compositions absorption in the range of 1.6 eV. These plots also clearly hint at currently limited absorption ranges that will be further discussed in section IV. As an upper limit, the maximum photocurrent density was estimated by integration of the AM1.5G spectrum with respect to the absorption onset, assuming that all photons above the band edge are converted with 100% efficiency and no parasitic absorption losses. Reported short-circuit current densities of highly efficient devices are often close to or surpass the theoretically predicted values. Negligence of capacitive effects in current-voltage measurements[50,51] or inaccuracies in the active device area that might be particularly severe for small device areas may lead to overestimation of the device performance. We here wanted to focus on cation alloying.

The data sets of the Cs-[5] and Rb-incorporating[6] metal halide perovskite devices are highlighted in Figure 4 showing that these values are at the forefront of state-of-the art metal halide perovskite device technology. In addition to these triple and quadruple cation compounds, we here also included recent results on Cs/FA[43,44] and Rb/FA[38] mixed dual-cation compounds as also in these cases, the clear benefit of the inclusion of alkine cations is evident but also mixed FA/MA cation alloys[34] exhibit their performance maximum at intermediate MA to FA ratios.
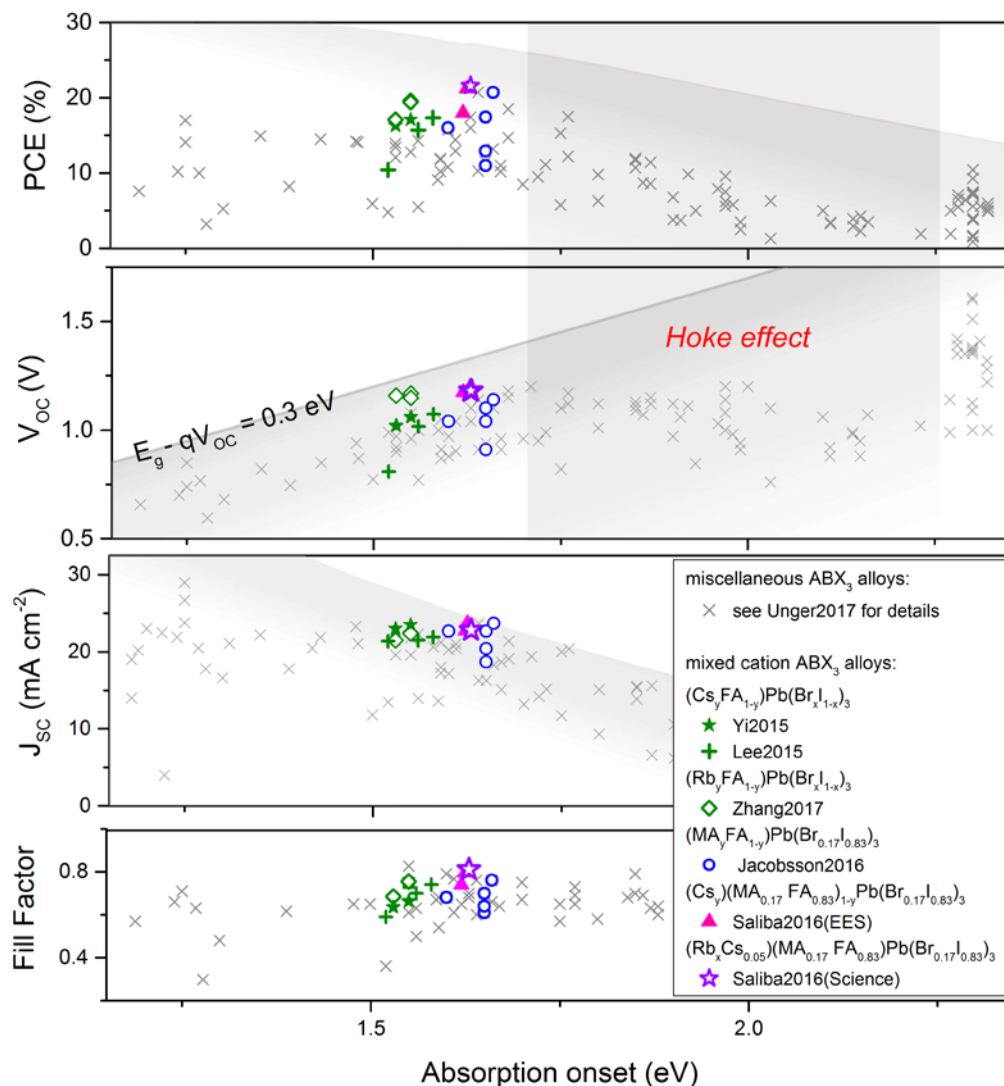
Figure 4: Device performance metrics of metal halide perovskite solar cells as a function of the absorption onset of the perovskite absorber showing data discussed elsewhere in grey[23] and highlighting devices based on cation alloys from data reported in [5,6,34,38,43,44] and are further discussed in Ref [23].

IV. CONCLUSION

The comparison of power conversion efficiencies as a function of the absorber layer onset for a variety of ABX_3 perovskite alloys highlights that there have been tremendous improvements in the obtained device efficiency in the past years due to chemical, compositional, process, and device engineering. As highlighted in this work, cation-alloys and particularly the

incorporation of small amount of alkaline cations have a beneficial effect on the device performance and durability. This approach has substantially improved the performance and reproducibility of single junction perovskite devices during this past year.

As evident in Figure 4 and further discussed in Unger et al.[23], metal halide perovskites can be tuned in a wide range of band gaps and substantial progress has been made both for low band gap devices, single junction devices with band gaps on the order of 1.6 eV and higher bandgap pure bromide compounds while there is a range between 1.7 and below the band gap of pure bromide derivatives of about 2.3 eV that can currently not be covered due to halide segregation.[9,26,27] These materials currently exhibit photo-induced phase segregation effects coined the "Hoke effect"[26] as halide vacancies are prone to form and have a low activation energy for migration. Apart from materials in the compositional range where photo-induced phase segregation is observed, the migration of halide and other ionic vacancies will be detrimental for the long-term stability of perovskite solar cells.[26,52]

While perovskite materials can often be tuned continously, phase segregation seems to be governed by ratios of ion radii. Thus, not every wide band gap material reported can be formed in such a way to permit continuous device operation without phase segregation as evidence statistically in previous works.[26,52] Only a limited amount of alkaline cations such as Cs can actually be included in predominantly hybrid perovskite materials comprising organic monovalent cations. More work comparing the vast and growing amount of literature data reported for metal halide perovskite semiconductors is needed to discuss generalizable trends of these emerging semiconductors to assess their potential and limitations.

ACKNOWLEDGEMENT

REFERENCES

(1) Kojima, A.; Teshima, K.; Shirai, Y.; Miyasaka, T. *J. Am. Chem. Soc.* **2009**, *131*, 6050–6051.

(2) Im, J.-H.; Lee, C.-R.; Lee, J.-W.; Park, S.-W.; Park, N.-G. *Nanoscale* **2011**, *3*, 4088–4093.

(3) Lee, M. M.; Teuscher, J.; Miyasaka, T.; Murakami, T. N.; Snaith, H. J. *Science (80-.).* **2012**, *3*, 1–5.

(4) Kim, H.-S.; Lee, C.-R.; Im, J.-H.; Lee, K.-B.; Moehl, T.; Marchioro, A.; Moon, S.-J.; Humphry-Baker, R.; Yum, J.-H.; Moser, J. E.; Grätzel, M.; Park, N.-G. *Sci. Rep.* **2012**, *2*, 591.

(5) Saliba, M.; Matsui, T.; Seo, J.-Y.; Domanski, K.; Correa-Baena, J.-P.; Mohammad K., N.; Zakeeruddin, S. M.; Tress, W.; Abate, A.; Hagfeldt, A.; Grätzel, M. *Energy Environ. Sci.* **2016**, *9*, 1989–1997.

(6) Saliba, M.; Matsui, T.; Domanski, K.; Seo, J.-Y.; Ummadisingu, A.; Zakeeruddin, S. M.; Correa-Baena, J.-P.; Tress, W. R.; Abate, A.; Hagfeldt, A.; Grätzel, M. *Science (80-.).* **2016**, *354*.

(7) Li, X.; Bi, D.; Yi, C.; Decoppet, J.-D.; Luo, J.; Zakeeruddin, S. M.; Hagfeldt, A.; Gratzel, M. *Science (80-.).* **2016**, *8060*, 1–10.

(8) Green, M. A.; Emery, K.; Hishikawa, Y.; Warta, W.; Dunlop, E. D.; Levi, D. H.; Ho-Baillie, A. W. Y. *Prog. Photovolt Res. Appl.* **2017**, *25*, 3–13.

(9) Noh, J. H.; Im, S. H.; Heo, J. H.; Mandal, T. N.; Seok, S. Il. *Nano Lett.* **2013**, *13*, 1764–1769.

(10) Eperon, G. E.; Leijtens, T.; Bush, K. a; Prasanna, R.; Green, T.; Wang, J. T.-W.; McMeekin, D. P.; Volonakis, G.; Milot, R. L.; May, R.; Palmstrom, a.; Slotcavage, D. J.; Belisle, R. a.; Patel, J. B.; Parrott, E. S.; Sutton, R. J.; Ma, W.; Moghadam, F.; Conings, B.; Babayigit, A.; Boyen, H.-G.; Bent, S.; Giustino, F.; Herz, L. M.; Johnston, M. B.; McGehee, M. D.; Snaith, H. J. *Science (80-.).* **2016**, *354*, 861–865.

(11) Eperon, G. E.; Stranks, S. D.; Menelaou, C.; Johnston, M. B.; Herz, L.; Snaith, H. *Energy Environ. Sci.* **2014**, *7*, 982–988.

(12) McMeekin, D. P.; Sadoughi, G.; Rehman, W.; Eperon, G. E.; Saliba, M.; Horantner, M. T.; Haghighirad, a.; Sakai, N.; Korte, L.; Rech, B.; Johnston, M. B.; Herz, L. M.; Snaith, H. J. *Science (80-.).* **2016**, *351*, 151–155.

(13) Loper, P.; Niesen, B.; Moon, S.-J.; Martin de Nicolas, S.; Holovsky, J.; Remes, Z.; Ledinsky, M.; Haug, F.-J.; Yum, J.-H.; De Wolf, S.; Ballif, C. *IEEE J. Photovoltaics* **2014**, *4*, 1545–1551.

(14) Albrecht, S.; Saliba, M.; Correa, P.; Lang, F.; Korte, L.; Schlatmann, R.; Nazeeruddin, M. K.; Hagfeldt, A.; Gra, M. *Energy Environ. Sci.* **2015**, *9*, 81–88.

(15) Bailie, C. D.; Christoforo, M. G.; Mailoa, J. P.; Bowring, A. R.; Unger, E. L.; Nguyen, W. H.; Burschka, J.; Pellet, N.; Nou, R.; Buonassisi, T.; Salleo, A. *Energy Environ. Sci.* **2015**, *8*, 956–963.

(16) Forgács, D.; Gil-Escrig, L.; Pérez-Del-Rey, D.; Momblona, C.; Werner, J.; Niesen, B.; Ballif, C.; Sessolo, M.; Bolink, H. J. *Adv. Energy Mater.* **2017**, 1602121.

(17) Albrecht, S.; Rech, B. *Nat. Energy* **2017**.

(18) Albrecht, S.; Saliba, M.; Correa-Baena, J.-P.; Jäger, K.; Korte, L.; Hagfeldt, A.; Grätzel, M.; Rech, B. *J. Opt.* **2016**, *18*, 064012.

(19) Bailie, C. D.; McGehee, M. D. *MRS Bull.* **2015**, *40*, 681–686.

(20) Werner, J.; Barraud, L.; Walter, A.; Bräuninger, M.; Sahli, F.; Sacchetto, D.; Tétreault, N.; Paviet-Salomon, B.; Moon, S.-J.; Allebé, C.; Despeisse, M.; Nicolay, S.; De Wolf, S.; Niesen, B.; Ballif, C. *ACS Energy Lett.* **2016**, 474–480.

(21) Beiley, Z. M.; McGehee, M. D. *Energy Environ. Sci.* **2012**, *5*, 9173–9178.

(22) Noh, J. H.; Im, S. H.; Heo, J. H.; Mandal, T. N.; Seok, S. Il. *Nano Lett.* **2013**, *13*, 1764–1769.

(23) Unger, E. L.; Kegelmann, L.; Suchan, K.; Sörell, D.; Korte, L.; Albrecht, A. *J. Mater. Chem. A* **2017**, *Advance Ar*.

(24) Weber, D. *Z. Naturforsch.* **1978**, *33b*, 1443–1445.

(25) Weber, D. *Z. Naturforsch.* **1978**, *33b*, 862–865.

(26) Hoke, E. T.; Slotcavage, D. J.; Dohner, E. R.; Bowring, A. R.; Karunadasa, H. I.; McGehee, M. D. *Chem. Sci.* **2014**, *6*, 613–617.

(27) Jeon, N. J.; Noh, J. H.; Yang, W. S.; Kim, Y. C.; Ryu, S.; Seo, J.; Seok, S. Il. *Nature* **2015**, *517*, 476–480.

(28) Zhao, B.; Abdi-Jalebi, M.; Tabachnyk, M.; Glass, H.; Kamboj, V. S.; Nie, W. A.; Pearson, J.; Puttisong, Y.; G??del, K. C.; Beere, H. E.; Ritchie, D. a.; Mohite, A. D.; Dutton, S. E.; Friend, R. H.; Sadhanala, A. *Adv. Mater.* **2017**, *29*, 1604744.

(29) Yang, Z.; Rajagopal, A.; Jo, S. B.; Chueh, C.; Williams, S.; Huang, C.; Katahara, J. K.; Hillhouse, H. W.; Jen, A. K. *Nano Lett* **2016**, *16*, 7739–7747.

(30) Zhao, D.; Yu, Y.; Wang, C.; Liao, W.; Shrestha, N.; Grice, C. R.; Cimaroli, A. J.; Guan, L.; Ellingson, R. J.; Zhu, K.; Zhao, X.; Xiong, R.-G.; Yan, Y. *Nat. Energy* **2017**.

(31) Kulbak, M.; Cahen, D.; Hodes, G. *J. Phys. Chem. Lett.* **2015**, *6*, 2452–2456.

(32)   Habisreutinger, S. N.; McMeekin, D. P.; Snaith, H. J.; Nicholas, R. J. *APL Mater.* **2016**, *4*.

(33)   Fedeli, P.; Gazza, F.; Calestani, D.; Ferro, P.; Besagni, T.; Zappettini, A.; Calestani, G.; Marchi, E.; Ceroni, P.; Mosca, R. *J. Phys. Chem. C* **2015**, *119*, 21304–21313.

(34)   Jacobsson, J. T.; Correa Baena, J. P.; Pazoki, M.; Saliba, M.; Schenk, K.; Grätzel, M.; Hagfeldt, A. *Energy Environ. Sci.* **2016**, *41*, 1–35.

(35)   Li, Z.; Yang, M.; Park, J.-S.; Wei, S.-H.; Berry, J.; Zhu, K. *Chem. Mater.* **2016**, *28*, 284–292.

(36)   Sutton, R. J.; Eperon, G. E.; Miranda, L.; Parrott, E. S.; Kamino, B. a.; Patel, J. B.; Hörantner, M. T.; Johnston, M. B.; Haghighirad, A. A.; Moore, D. T.; Snaith, H. J. *Adv. Energy Mater.* **2016**, *6*, 1–6.

(37)   Beal, R. E.; Slotcavage, D. J.; Leijtens, T.; Bowring, A. R.; Belisle, R. A.; Nguyen, W. H.; Burkhard, G.; Hoke, E. T.; McGehee, M. D. *J. Phys. Chem. Lett.* **2016**, 746–751.

(38)   Zhang, M.; Yun, J. S.; Ma, Q.; Zheng, J.; Fai, C.; Lau, J.; Deng, X.; Kim, J.; Kim, D.; Seidel, J.; Green, M. A.; Huang, S.; Ho-baillie, A. W. Y. **2017**.

(39)   Sadhanala, A.; Deschler, F.; Thomas, T. H.; Dutton, S. E.; Goedel, K. C.; Hanusch, F. C.; Lai, M. L.; Steiner, U.; Bein, T.; Docampo, P.; Cahen, D.; Friend, R. H. *J. Phys. Chem. Lett.* **2014**, *5*, 2501–2505.

(40)   Hao, F.; Stoumpos, C. C.; Cao, D. H.; Chang, R. P. H.; Kanatzidis, M. G. *Nat. Photonics* **2014**, *8*, 489–494.

(41)   Goldschmidt, V. M. *Naturwissenschaften* **1926**, *14*, 477–485.

(42)   Kieslich, G.; Sun, S.; Cheetham, T. *Chem. Sci.* **2015**, *6*, 3430–3433.

(43)   Lee, J.-W.; Kim, D.-H.; Kim, H.-S.; Seo, S.-W.; Cho, S. M.; Park, N.-G. *Adv. Energy Mater.* **2015**, *5*, 1501310.

(44)   Yi, C.; Luo, J.; Meloni, S.; Boziki, A.; Ashari-Astani, N.; Grätzel, C.; Zakeeruddin, S. M.; Röthlisberger, U.; Grätzel, M. *Energy Environ. Sci.* **2016**, *9*, 656–662.

(45)   Choi, H.; Jeong, J.; Kim, H.-B.; Kim, S.; Walker, B.; Kim, G.-H.; Kim, J. Y. *Nano Energy* **2014**, *7*, 80–85.

(46)   Umebayashi, T.; Asai, K.; Kondo, T.; Nakao, A. *Phys. Rev. B* **2003**, *67*, 155405.

(47)   Brivio, F.; Walker, A.; Walsh, A. *APL Mater.* **2013**, *1*, 042111.

(48)   Matsui, T.; Seo, J.; Saliba, M.; Zakeeruddin, S. M.; Grätzel, M. **2017**, 2–6.

(49)   Philippe, B.; Saliba, M.; Cappel, U. B.; Gra, M. **2017**.

(50)   Christians, J. A.; Manser, J. S.; Kamat, P. V. *J. Phys. Chem. Lett.* **2015**, *6*, 852–857.

(51)   Unger, E. L.; Hoke, E. T.; Bailie, C. D.; Nguyen, W. H.; Bowring, A. R.; Heumuller, T.; Christoforo, M. G.; McGehee, M. D. *Energy Environ. Sci.* **2014**, *7*, 3690–3698.

(52)   Slotcavage, D. J.; Karunadasa, H. I.; McGehee, M. D. *ACS Energy Lett.* **2016**, 1199–1205.

(53)   Green, M. a.; Jiang, Y.; Soufiani, A. M.; Ho-Baillie, A. *J. Phys. Chem. Lett.* **2015**, *6*, 4774–4785.

(54)   Saba, M.; Quochi, F.; Mura, A.; Bongiovanni, G. *Acc. Chem. Res.* **2015**, *49*, 166–173.

ADDITIONAL COMMENTS

[i] *The reader should note that experimental data is compared as a function of the absorption onset rather than the band gap as the latter is indeed not directly available from experimental data in materials with excitonic contributions to the spectrum close to the band gap as is the case for metal halide perovskites.*[53,54]

[ii] *Note that the trend for Cs-incorporating MA/FA alloys (points K-N in Figure 2, right) closely correspond with the predicted trend unlike the statement first made in the original paper as we realized during the work on this manuscript that the estimated values for the lattice parameter a_0 were faulty. A correction was send to point out this mistake in the original manuscript.*[23]